

Superconductivity, intergrain and intragrain critical current densities of $Tl_2Ca_2Ba_2Cu_3O_{10+\delta}$ and $Tl_2CaBa_2Cu_2O_{8+\delta}$ materials

J. R. Thompson

*Solid State Division, Oak Ridge National Laboratory, P.O. Box 2008, Oak Ridge, Tennessee 37831-6061
and Department of Physics, University of Tennessee, Knoxville, Tennessee 37996-1200*

J. Brynestad

Chemistry Division, Oak Ridge National Laboratory, P.O. Box 2008, Oak Ridge, Tennessee 37831-6100

D. M. Kroeger

Metals and Ceramics Division, Oak Ridge National Laboratory, P.O. Box 2008, Oak Ridge, Tennessee 37831-6116

Y. C. Kim

Department of Physics, University of Tennessee, Knoxville, Tennessee 37996-1200

S. T. Sekula and D. K. Christen

Solid State Division, Oak Ridge National Laboratory, P.O. Box 2008, Oak Ridge, Tennessee 37831-6061

E. D. Specht

Metals and Ceramics Division, Oak Ridge National Laboratory, P.O. Box 2008, Oak Ridge, Tennessee 37831-6116

(Received 12 September 1988)

Bulk sintered and powdered samples of the high-temperature superconductive compounds $Tl_2Ca_2Ba_2Cu_3O_{10+\delta}$ (Tl-2:2:2:3) and $Tl_2CaBa_2Cu_2O_{8+\delta}$ (Tl-2:1:2:2) have been synthesized with phase purity of approximately 90%. The materials were characterized by x-ray-diffraction, metallographic, and electron microprobe analyses. The electronic and superconductive properties were investigated through measurement of the electrical resistivity and the critical current density J_c using transport methods and by extensive magnetization measurements. Primary results and conclusions are that (1) the intragrain J_c values were large, much larger than the transport values; (2) both sintered and powdered materials exhibited large flux creep; (3) and the J_c decreased exponentially with temperature. These features are qualitatively very similar to those found in the corresponding $YBa_2Cu_3O_z$ (with $z \approx 7$) series of compounds.

I. INTRODUCTION

During the past two years, great advances have been made in the area of high-temperature superconductivity. Most notably, the superconductive transition temperature T_c has been pushed upward by a factor of 5 or more, relative to the previously available materials. There are now several families of materials exhibiting well-documented superconductivity at temperatures above 30 K, nearly all of which are based on layered copper oxide structures: the $La_{1-x}Sr_xCuO_4$ compounds with T_c near 40 K; the "1:2:3" set of $R_1Ba_2Cu_3O_z$ materials with $z \approx 7$, where R denotes Y or most elements in the 4f series; a family of superconductors based on Bi-Sr-Ca-Cu oxides; and a group of layered compounds of the type Tl-Ca-Ba-Cu oxide. Discovery of the Tl-based superconductors by Sheng and Hermann¹ has provided an alternate set of compounds in which many concepts and models that were devised for 1:2:3 materials can be tested and the substances compared.

One area of particular concern for potential applications of high- T_c superconductors (HTSC) is the current carrying capacity, which is crucial for nearly every usage of bulk materials. Thus, both qualitative and quantitative

information on the critical current density $J_c(H, T)$ attainable in a magnetic field H at temperature T is of primary importance. In the widely studied 1:2:3 series, it has been found almost without exception that the transport J_c values in bulk, sintered specimens are quite modest in magnitude and very much smaller than the J_c 's deduced from measurements of irreversibility in the magnetization. The general explanation is that these two methods are sensitive to supercurrents between grains and within grains, respectively, with substantial weak-link barriers at interfaces that decouple the sintered particles. The origin(s) of the barriers is not certain, but various explanations include nonstoichiometric or glassy material at grain boundaries, the accumulation of impurities at these boundaries, and the presence of twin boundaries. The last possibility arose because the problem of decoupling first became apparent in orthorhombic Y-1:2:3, where twinning is very prevalent. With the availability of Tl-based HTSC compounds, it is important to assess whether they suffer from these same problems. Since most of the Tl-based compounds are tetragonal in structure²⁻⁵ and therefore less subject to twinning, a contrasting case for the role of twin planes can be investigated.

In this study, we have synthesized powdered and bulk

sintered samples of $\text{Tl}_2\text{Ca}_2\text{Ba}_2\text{Cu}_3\text{O}_{10+\delta}$ (Tl-2:2:2:3) and $\text{Tl}_2\text{CaBa}_2\text{Cu}_2\text{O}_{8+\delta}$ (Tl-2:1:2:2) with relatively high phase purity and have made magnetic and resistive investigations of the superconductive transition. The intergranular critical current density was measured as a function of magnetic field at 77 K; for contrast, the intragranular J_c was determined from 4.2 to 77 K in fields up to 78 kOe. Comparison of the two sets of measurements shows that these sintered Tl-based samples exhibit the same weak coupling between grains that has characterized sintered 1:2:3 materials.

II. EXPERIMENTAL ASPECTS

A. Synthesis

A typical procedure was as follows: The materials were prepared by weighing appropriate amounts of dried, high-purity powders of Tl_2O_3 , CaO , BaO , and CuO (with the oxides of Ca and Ba being prepared in our laboratory). The components, with a gross composition of $\text{Tl}_2\text{Ca}_2\text{Ba}_2\text{Cu}_3\text{O}_{10+\delta}$ (Tl-2:2:2:3), were thoroughly mixed in a mortar and loaded into a $\frac{1}{2}$ -in.-diameter steel die. These procedures were performed in a helium drybox with less than $\frac{1}{2}$ ppm H_2O . After the powder was pressed into a pellet at ~ 4000 kg/cm², it was removed from the drybox and quickly loaded into a gold capsule that was then welded shut. For reaction, the capsule was first heated quickly to $\sim 750^\circ\text{C}$ and held there for 16 h. It was observed that the capsule bulged out, indicating a considerable pressure of $\text{Tl}_2\text{O} + \text{O}_2$ gases during initial stages of the process. The capsule was subsequently heated to 850°C for 16 h, whereupon it was cooled, and the pellet reground (in dry air), repressed, resealed into a gold capsule, and reheated to 850°C for ~ 16 h. In the case of the sample Au4-7, this procedure was performed six times. Between each regrinding, a "sliver" of the sample was investigated with respect to T_c and x-ray-diffraction patterns. After the first heating, the sample (Au4-1) consisted mainly of a mixture of $\text{Tl}_2\text{Ba}_2\text{CuO}_6$ (Tl-2:0:2:1) and $\text{Tl}_2\text{CaBa}_2\text{Cu}_2\text{O}_8$ (Tl-2:1:2:2), with a small amount of Tl-2:2:2:3. The proportion of Tl-2:2:2:3 increased after each reheating until the fifth time (Au4-6). Further processing yielded material (sample Au4-7) that was practically identical to Au4-6. It also was observed that subsequent annealing in 1 atm O_2 at 560°C for 1 h or more greatly sharpened the superconducting transition of the samples, but did not change the x-ray powder pattern. The sample gained weight during the treatment in oxygen, so the compositions are written as $\text{Tl}_2\text{Ca}_2\text{Ba}_2\text{Cu}_3\text{O}_{10+\delta}$ and $\text{Tl}_2\text{CaBa}_2\text{Cu}_2\text{O}_{8+\delta}$ where δ is small and positive in each case. It seems to be a safe conclusion that the compound Tl-2:2:2:3 is stable at 850°C , although initially other phases are formed when one starts with the gross composition of Tl-2:2:2:3.

The Tl-2:1:2:2 materials were prepared using similar methods. Additional details of synthesis are included in a report on the structure of this compound.⁶ A portion of this same Tl-2:1:2:2 powder has been used for the present investigations of the magnetically measured critical current density.

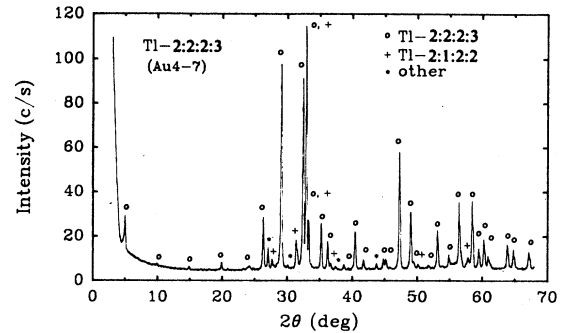


FIG. 1. Powder x-ray-diffraction pattern of sample Au4-7. $\text{Tl}_2\text{Ca}_2\text{Ba}_2\text{Cu}_3\text{O}_{10+\delta}$ peaks are labeled with a "○", $\text{Tl}_2\text{CaBa}_2\text{Cu}_2\text{O}_{8+\delta}$ with a "+". Other peaks labeled "*": peak at $2\theta = 30.15^\circ$ is $\text{Tl}_2\text{Ba}_2\text{CuO}_{6+\delta}$; $2\theta = 37.35^\circ$ is CaO ; peaks at $2\theta = 27.07^\circ$ and 43.75° are unassigned.

B. X-ray diffraction

We used powder x-ray diffraction to identify the phases in the samples. Scans were taken on a Norelco diffractometer equipped with a copper target and a graphite diffracted beam monochromator tuned to $\text{Cu } K\alpha$, and operated at 700 W. Figure 1 indicates assignments of prominent peaks in sample Au4-7. The dominant phase is $\text{Tl}_2\text{Ca}_2\text{Ba}_2\text{Cu}_3\text{O}_{10+\delta}$, giving diffraction consistent with the structure of Ref. 2. A second phase agrees with the structure $\text{Tl}_2\text{CaBa}_2\text{Cu}_2\text{O}_{8+\delta}$ (Ref. 3). A single peak for each phase suggests the presence of $\text{Tl}_2\text{Ba}_2\text{CuO}_{6+\delta}$ (Ref. 5) and CaO . Two peaks must be attributed to an unidentified phase.

C. Materials characterization

Four-terminal resistive critical-current-density measurements were made at 77 K in liquid nitrogen with an applied magnetic field perpendicular to the sample axis. Current contacts were made by first wetting the ends of the sample with a liquid metal alloy containing Hg, Tl, and In and then pressing the specimen lengthwise between copper contacts to which were tinned thick indium pads. Deformation of the indium pads provided maximum contact area. The voltage contacts were 1 cm apart and a voltage criterion for J_c of $5 \mu\text{V}$ was used.

The magnetic measurements were performed in a laboratory-constructed vibrating sample magnetometer equipped with a Nb-Ti and Nb_3Sn hybrid superconducting solenoid that was used to generate magnetic fields up to 80 kOe. For measurement of the sample temperature, calibrated Si-diode and carbon glass resistance sensors were used.

III. EXPERIMENTAL RESULTS

A. The superconductive transition

The transition to the superconductive state was investigated primarily by magnetic methods. In addition, the

electrical resistivity $\rho(T)$ of bulk sintered samples was measured as a function of temperature. As an example, for the Tl-2:2:2:3 sample designated Au4-7, the resistivity varied linearly in the temperature interval between room temperature (with $\rho = 1.45 \text{ m}\Omega \text{ cm}$ at 273 K) and approximately 160 K, then decreased more rapidly at lower temperature. The midpoint of the resistive transition was 125 K with the resistance becoming immeasurably small at 124 K. In Fig. 2 are shown for the same sample complementary magnetic measurements of the normalized low-field dc susceptibility $4\pi\chi$, using a static measuring field of 3.6 Oe. The results in this expanded plot were obtained (1) by field cooling (FC) the sample in the applied field (triangles), thereby measuring the flux expulsion corresponding to a true Meissner Effect; and (2) by zero-field cooling (ZFC) to 4.2 K, after which the desired field was applied (circles). The diamagnetic onset T_c of 125 K coincides well with the resistive value. The FC transition is relatively sharp, with a width (10% to 90%) of 2.3 K. On the other hand, the ZFC curve exhibits a step at lower temperature and appears to have two transitions. This is explained by the fact that this signal arises from shielding of the sample volume, due to induced macroscopic shielding currents that flow near the surface of the material; at low temperature, we have $4\pi\chi = -0.98$, corresponding to nearly complete screening of the interior. However, the intergranular dc screening currents can persist only so long as the critical current density J_c between grains is not exceeded. With increasing temperature, this J_c decreases, such that the grains become decoupled at some temperature depending on the applied field. This causes the ZFC signal to decrease rapidly in magnitude (near 120 K in Fig 2) until it assumes a value that, for these materials, is quite comparable to the FC Meissner susceptibility. In Fig. 2, the decoupling temperature T_d , defined as that at which the grains are completely decoupled, is 123.7 K. The temperature dependence of the ZFC susceptibility in various applied fields from 1.3 to 109 Oe is shown in Fig. 3 for sample Au4-7. Noteworthy is the fact that decoupling occurs at progressively lower temperatures for larger fields. The magnitude of the susceptibility $4\pi\chi$ remaining after decoupling was nearly the same, about -0.3 , for

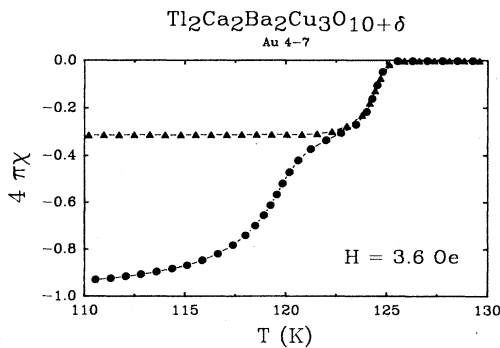


FIG. 2. The normalized magnetic susceptibility $4\pi\chi$ vs temperature T for a sintered sample of $\text{Tl}_2\text{Ca}_2\text{Ba}_2\text{Cu}_3\text{O}_{10+\delta}$. Measurements were made while FC in an applied field of 3.6 Oe (\blacktriangle), and by cooling in zero applied field (ZFC) to low temperature, after which the field was applied (\bullet).

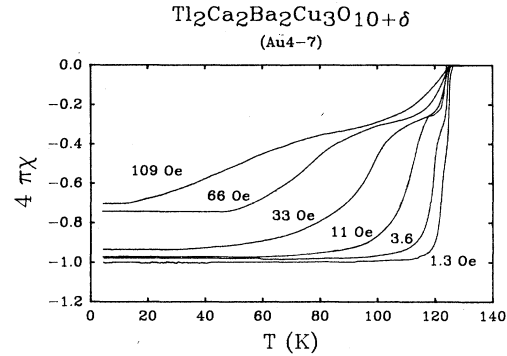


FIG. 3. The normalized, zero-field cooled susceptibility $4\pi\chi$ vs temperature in various magnetic fields, for the same $\text{Tl}_2\text{Ca}_2\text{Ba}_2\text{Cu}_3\text{O}_{10+\delta}$ sample as Fig. 2. Note the steps corresponding to decoupling of grains that occur at progressively lower decoupling temperatures T_d .

each of the fields used. The relationship between decoupling temperature T_d and applied magnetic field H , shown in Fig. 4, appears to be approximately linear over the range of data; other dependencies are possible, however. The figure shows that rather modest fields tend to decouple the grains. This is a direct consequence, in our opinion, of the relatively low intergrain critical current density in the sintered samples, as is sensed in a transport measurement of J_c and will be discussed below. For now, we note that the decoupling temperature is determined by the temperature dependencies of both J_c and an effective penetration depth.

The penetration depth also has a strong influence on other observed properties of these materials. In particular, the magnitude of the normalized susceptibility $4\pi\chi$, either the FC or ZFC value, is often equated to the superconductive volume fraction in the sample. This ignores the fact that in powdered samples a significant portion of a grain's volume can be penetrated by the measuring field (assuming $H < H_{c1}$), as discussed by Clem and Kogan.⁷ As a consequence, the susceptibility is reduced in magnitude. Similar phenomena can occur in sintered samples since the grains are easily decoupled by the measuring field, thereby requiring care in the interpretation of such data.⁸ However, this effect also affords the possibility of

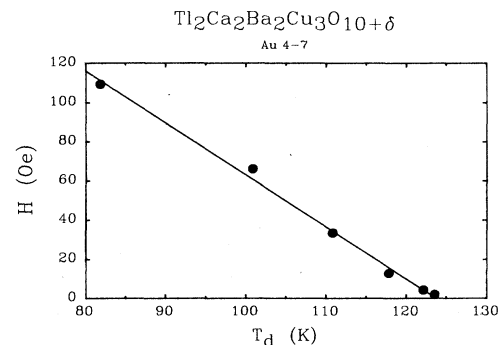


FIG. 4. The relationship between applied magnetic field H and temperature T_d at which sintered grains become decoupled.

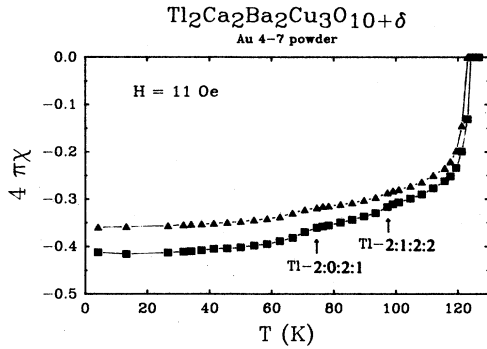


FIG. 5. The susceptibility $4\pi\chi$ vs temperature of powdered $\text{Tl}_2\text{Ca}_2\text{Ba}_2\text{Cu}_3\text{O}_{10+\delta}$, in FC (\blacktriangle) and ZFC (\blacksquare) measurements. Contributions due to Tl-2:1:2:2 and Tl-2:0:2:1 impurity phases are noted.

determining the penetration depth $\lambda(T)$. For example, measurements on axially aligned, dispersed powders of Tl-2:2:2:3 have shown that the penetration is anisotropic as expected for these layered materials. Using the observed susceptibility $4\pi\chi$ at 4.2 K and the measured particle size distribution, we obtain preliminary values for the penetration depths with λ_c ($\approx 9 \mu\text{m}$) an order of magnitude larger than λ_{ab} ($\approx 0.9 \mu\text{m}$). Here the subscript c (ab) refer to the direction of supercurrents along c (ab) that screen an externally applied field $H < H_{c1}$ from the interior of a superconducting grain. In axially aligned $\text{YBa}_2\text{Cu}_3\text{O}_z$ powders, a similar analysis⁹ yielded the values $\lambda_{ab} \approx 0.27 \mu\text{m}$ and $\lambda_c = 1.2 \mu\text{m}$. Compared with Y-Ba-Cu-O, both the magnitudes and anisotropy of λ for Tl-2:2:2:3 are greater, which is plausible given the more extreme layering of the latter material. However, the temperature dependence of $\chi(T)$ for Tl samples, such as that shown in Fig. 5, differed significantly from either conventional two fluid or BCS results. Until these and other questions are resolved by further investigations, values for λ in the Tl-based compound must be viewed as preliminary results.

Another factor influencing the Meissner (FC) signal is pinning of magnetic flux lines in the superconductor, which reduces the realized flux expulsion. However, for the Tl-based materials investigated to date, we find that the low-field susceptibility is relatively reversible. For example, in measurements on powdered Tl-2:2:2:3 materials as shown in Fig. 5, the values of $4\pi\chi$ at 4.2 K were -0.36 and -0.42 for the FC and ZFC cases, respectively. Hence, penetration depth effects provide the major mechanism whereby the signal is diminished in this case. We also note that these magnetic measurements revealed the presence of superconductive minority phases, approximately 10% by volume, in semiquantitative agreement with microprobe and x-ray-diffraction analyses of the samples.

B. Transport critical current density: intergranular J_c

The transport critical current density J_c of bulk, sintered, Tl-based materials was measured using dc current

while the samples were immersed in liquid nitrogen. Figure 6 shows the resistively measured critical current-density J_c at 77 K as a function of magnetic field H up to 10 kOe for the sample designated Au4-7. These results are typical of those obtained for several specimens with different heat treatments, including the sintered Tl-2:1:2:2 specimen from which powder was made for the measurements in Sec. III C and have several features in common with $J_c(H)$ curves for Y-1:2:3 sintered material. The rapid decrease of J_c at very low applied fields and the generally low values of J_c have, in the Y-1:2:3 material, been taken as evidence for the presence of "weak links" or non-superconducting barriers to current flow.¹⁰ Magnetically derived critical current densities discussed below suggest that the weak links in this material are, as in sintered Y-1:2:3, at grain boundaries. The values of J_c at 1.5–5.0 kOe are substantially higher than is typical of sintered Y-1:2:3 material with randomly oriented grains. For the Tl-2:1:2:2 sample that was later powdered, the maximum in J_c came at ~ 1.8 kOe and the maximum J_c was 310 A/cm^2 .

The dependence of the transport J_c on externally applied field H (Fig. 6) can be compared with recent "weak-link" models that provide a rapid decrease in J_c with field. For a simple Josephson-coupled junction, the critical current density $J_c(H)$ in a field follows a simple Fraunhofer diffraction with $J_c(H)/J_c(0) = |\sin(\pi H/H_0)|/(\pi H/H_0)$. The characteristic field H_0 corresponds to threading one quantum of flux ϕ_0 through the junction area dL , where L is the length of the junction and $d = (2\lambda + w)$ is its width, with λ being the penetration depth. This follows the notation of Petersen and Ekin.¹¹ As shown by those authors, an averaging over angle and junction area smears out the zeros of this simple function and results in a field dependence where J_c decreases slightly faster than $1/H$. (See Fig. 4 in Ref. 11, for example, and Ref. 12.) A similar relationship is exhibited by the data in Fig. 6, where the broken line is drawn with

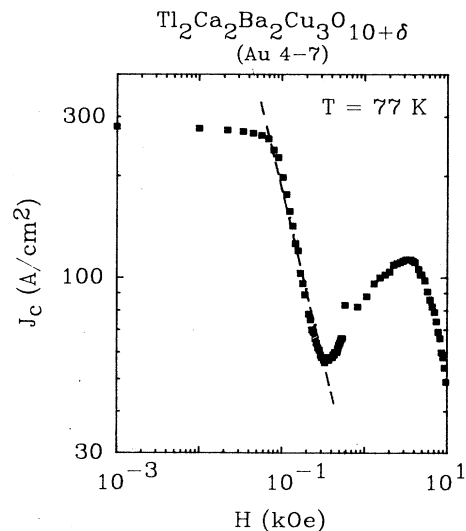


FIG. 6. The transport critical current-density J_c of Tl-2:2:2:3 sample Au4-7 at 77 K vs magnetic field H . The dashed line indicates a $1/H$ dependence.

$J_c \propto 1/H$ and the experimental data are slightly steeper. This is strongly suggestive of weak-link limitations in these Tl-based samples.

In very small external fields, it frequently is the case that the self-field created by the measuring current significantly affects the observed J_c value. In fact, Stephens¹² and Dersch and Blatter¹³ have argued that for nearly all macroscopic polycrystalline samples, this geometry-dependent mechanism limits the observed J_c values in very small fields. For our cylindrical specimen with 0.45 cm diameter, the observed J_c of 290 A/cm² corresponds to a self-field at the surface of 40 Oe. Hence, the application of external fields $H \leq 40$ Oe is expected to have relatively little influence on J_c and this is exactly what is observed in Fig. 6. This value roughly marks the change from a regime of self-field-limited J_c 's to one dominated by the external field where $J_c \propto 1/H$.

These observations are consistent with the ZFC magnetization results in Fig. 3. At a fixed temperature of 77 K, the normalized susceptibility $4\pi\chi$ begins to deviate noticeably from its low temperature value for $H \approx 33$ Oe, corresponding to an onset of decoupling between grains. (Note that the $H-T_d$ boundary in Fig. 4 corresponds to complete decoupling between grains.) Thus, both the susceptibility and transport J_c measurements show that at 77 K, external fields of 30–40 Oe initiate intergrain decoupling.

Although an analysis based on weak-link models explains some features of the $J_c(H)$ data, other aspects are difficult to understand in this context. Most notably, these include (1) the minimum in J_c followed by a maximum at still higher fields, as discussed below; and (2) the magnitude of the characteristic field H_0 in the Fraunhofer relation for $J_c(H)$. The data in Fig. 6 yield values for H_0 of 100–300 Oe, depending on the criterion employed. These values are roughly an order of magnitude larger than those found in sintered Y-Ba-Cu-O samples and correspond to an effective junction area dL of $(7-20) \times 10^{-10}$ cm². Assuming¹¹ that L is given by the mean grain size of ~ 5 μ m, one finds for the effective junction width $d \approx (2\lambda + w)$ the approximate values of $(1.4-4.0) \times 10^{-6}$ cm. This is very much smaller than either the preliminary values for λ in Tl-2:2:2:3 reported above or those found in Y-Ba-Cu-O materials. Consequently, it is difficult to make an exact one-to-one correspondence with the earlier physical picture¹¹ used for Y-Ba-Cu-O. One can speculate that these relatively porous Tl-based materials may contain *small* regions with relatively strong intergrain coupling and dimensions commensurate with the values of H_0 . This would be consistent with the large transport J_c 's observed in some dense, polycrystalline thin films and discussed in Sec. IV below.

Other difficulties with the weak link interpretation and two of the most striking features of Fig. 6 are the sharp minimum in J_c at ~ 350 Oe, and the broad maximum at ~ 3500 Oe. All of the Tl-based samples measured have shown these features, although the fields at which they occur vary. Sintered Y-1:2:3 material behaves similarly, but the minima and maxima tend to be more shallow and to occur at lower magnetic fields. Among the five Tl-based samples on which we have made resistive J_c measurements, the field at the J_c minimum has varied from

$\sim 130-500$ Oe, and the field at the maximum from 1700–3500 Oe. The cause of this field dependence is not known. In metallic superconductors maxima in $J_c(H)$ at fields well below H_{c2} can arise from matching of the spacing $a_0 = (2\phi_0/\sqrt{3}B)^{1/2}$ between flux lines with the average spacing between pinning sites; here B is the macroscopic average flux density in the material. J_c maxima due to this mechanism at 1700–3500 Oe would require pinning sites with average spacings of 1200–800 Å. However, if the initial rapid decrease of J_c is due to exceeding the critical current of weak links, it seems unlikely that an increase in bulk pinning due to matching would cause the maximum.

C. Magnetic critical current density: intragranular J_c

The critical current density was investigated magnetically using the Bean method¹⁴ in applied magnetic fields $H \gg H_{c1}$, for both sintered and powdered materials. In this method, J_c (in A/cm²) is given by the expression

$$J_c(H, T) = 15\Delta M/R, \quad (1)$$

where $\Delta M = (M_+ - M_-)$ is the hysteretic difference in sample magnetization M (in units of Gauss) measured in increasing versus decreasing field. The factor R is a characteristic transverse dimension, in units of cm. For powdered materials, R is of the order of the grain radius (or perhaps somewhat smaller); in sintered samples where the applied field has decoupled particles, it is apparent that the appropriate dimension is again of this magnitude. The mean grain size in sintered rods was obtained using a grain boundary intercept method applied to photographs of metallographic specimens illuminated with polarized light; values of R near 2.5 μ m were typical. To obtain the magnetization, the field sweep (108 Oe/s) was stopped periodically in order that the sample could reach a quasiequilibrated condition. As in earlier studies of La_{1-x}Sr_xCuO₄ materials,¹⁵ very substantial flux creep¹⁶ was observed especially at higher temperatures, such that the static values of M were considerably diminished from the dynamic values. This is illustrated for Tl-2:2:2:3 at a temperature of 60 K in Fig. 7 showing the magnetization

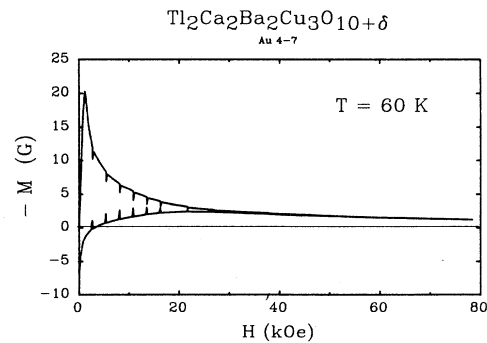


FIG. 7. The magnetization $-M$ of Tl-2:2:2:3 sample Au-4-7 at 60 K vs field H . The vertical spikes, formed when the field sweep was halted, are due to flux creep.

as a function of applied field H . The vertical spikes on the continuous curve were formed when the field sweep was stopped periodically to allow the sample to equilibrate. Only static values of M have been used for the following discussion.

The results of this analysis are a family of curves of J_c as a function of magnetic field H at fixed temperatures T . These are shown in Fig. 8 for Tl-2:2:2:3 and in Fig. 9 for Tl-2:1:2:2, respectively, and represent the critical current density within single crystallites, i.e., the intragranular J_c . Qualitatively, these J_c values are several orders of magnitude larger than those obtained by transport measurements. The intragrain J_c 's lie in the range of 10^6 – 10^7 A/cm² at 4.2 K for applied fields of a few tens of kOe, behavior that is typical of the Y-1:2:3 materials also. At low temperature, there is little dependence on the applied field up to 80 kOe while at higher temperature, a quite substantial diminution of J_c is observed with increasing H . Analogous effects were observed in similar studies on Fe-substituted $\text{YBa}_2(\text{Cu}_{1-x}\text{Fe}_x)_3\text{O}_z$ materials.¹⁷ In $\text{YBa}_2\text{Cu}_3\text{O}_7$, the field dependence at higher temperatures has been attributed¹⁸ to the influence of the upper critical field H_{c2} .

We now consider the temperature dependence of the intragranular current density. Values of J_c obtained in an applied field of 2.7 kOe have been chosen so as to minimize the influence of the upper critical field and are presented for Tl-2:2:2:3 and Tl-2:1:2:2 in Fig. 10 as a function of temperature T . The linear plot on the semi-logarithmic scale shows that J_c decreases exponentially with temperature

$$J_c(T) = J_c(0) \exp(-T/T_0), \quad (2)$$

where the factor T_0 is an empirical, characteristic temperature. Such a dependence was first observed in high-temperature superconductors by Finnemore *et al.*¹⁹ and has been discussed more recently by Senoussi *et al.*²⁰ While the theoretical basis for such a relationship is unclear, we note that explanations based on tunneling between grains are unlikely, since these effects have been observed in dispersed fine powders¹⁷ and single crystals²⁰ as

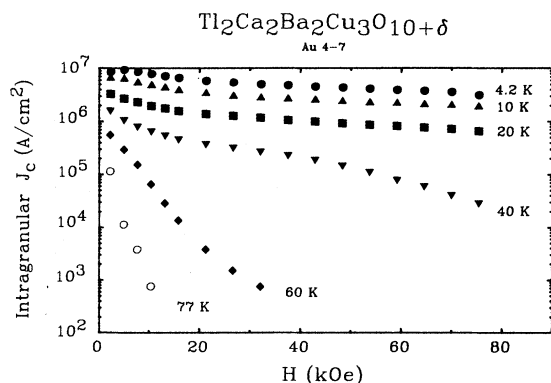


FIG. 8. The intragranular critical current-density J_c , determined magnetically, of Tl-2:2:2:3. Data are shown as a function of magnetic field H at various temperatures T .

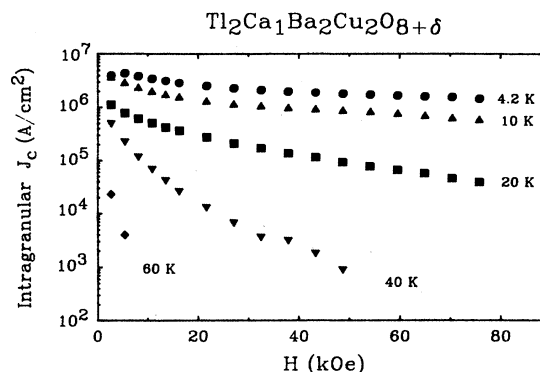


FIG. 9. The intragranular J_c of powdered Tl-2:1:2:2; otherwise, same as Fig. 8.

well as sintered samples. It is also improbable that mechanisms dependent on twinning, which might produce tunneling barriers at twin planes, can account for Eq. (2), since both the Tl-2:2:2:3 and Tl-2:1:2:2 compounds have tetragonal structures, in which twinning is much less prevalent than in the easily twinned orthorhombic structure of the $\text{YBa}_2\text{Cu}_3\text{O}_7$ family of materials. Additional evidence that twinning is unlikely to account for the behavior of the intragrain J_c was provided by studies of Fe-substituted Y-1:2:3 materials,¹⁷ wherein the lattice is driven toward tetragonality with the addition of Fe, leading to a disappearance of macroscopic twinning. In this study also, the current density decreased exponentially with temperature as given by Eq. (2). While a detailed explanation is not presently available, we may speculate that the temperature dependence of J_c is associated with giant flux creep,¹⁶ since this phenomenon, along with cupric oxide-layered structures, is one of the few physical features common to the several families of high- T_c materials.

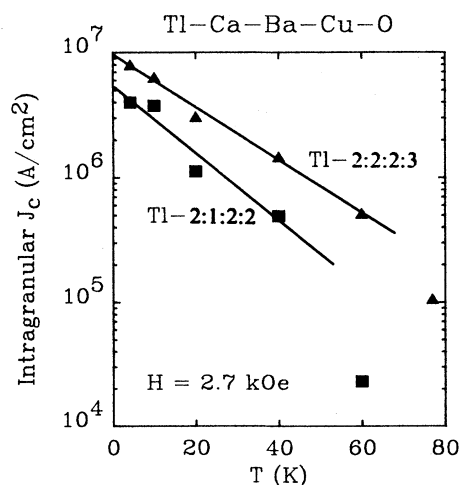


FIG. 10. The intragrain J_c in low applied fields (2.7 kOe) vs temperature T , for Tl-2:2:2:3 and Tl-2:1:2:2 materials, showing an exponential dependence $J_c(T) = J_c(0) \exp(-T/T_0)$; see text.

IV. DISCUSSION AND CONCLUSIONS

This study of Tl-based superconductive materials with the 2:2:2:3 and 2:1:2:2 compositions (Tl-Ca-Ba-Cu-oxides) revealed several features that are very similar to the $\text{YBa}_2\text{Cu}_3\text{O}_z$ family of compounds. Most striking is the fact that in the sintered samples investigated, the current densities determined by transport and by magnetic hysteresis measurements differ by several orders of magnitude; e.g., the intergranular J_c at 77 K is about 10^{-2} – 10^{-3} smaller than the intragranular J_c , as can be seen by comparison of Figs. 6 and 8. The limited intergrain current density is responsible as well for the loss of shielding susceptibility and the decoupling of grains that is discussed above in Sec. IIIA. Similar effects in the ZFC susceptibility have been observed in Y and rare-earth-based "1:2:3" materials. Thus, we have developed synthesis protocols leading to materials with relatively high phase purity and few nonsuperconductive inclusions. Unfortunately, the samples are very similar to the better known 1:2:3 family, in that they exhibit the same poor coupling between crystallites that limits current transport. Similar findings have been reported previously by Küpfer *et al.*²¹ based on ac permeability studies of multiphase Tl-2:2:2:3 samples. Comparison with the critical current values reported there reveals intragranular J_c 's quite similar to the present results, with magnitudes that seem to be characteristic of many high- T_c materials to date; the earlier transport values²¹ are somewhat lower but comparable. In this context, it was recently reported²² that, for thin-film Tl-2:1:2:2 samples, the J_c values obtained by pulsed current measurements exceeded those obtained magnetically, especially in substantial fields. Coupled with the large J_c 's that were relatively insensitive to fields of tens of kOe, these results are intriguing in that the magnetization exhibited giant flux creep similar to that observed in the current work. The influence of this temporal phenomenon, flux creep, on the ultimately attainable critical current density in high-temperature superconductive materials is unclear at this time.

Another similarity between these Tl-based sintered materials and their Y-1:2:3 counterparts is the exponential dependence of J_c on temperature. Since this relationship has been found frequently for bulk specimens of HTSC

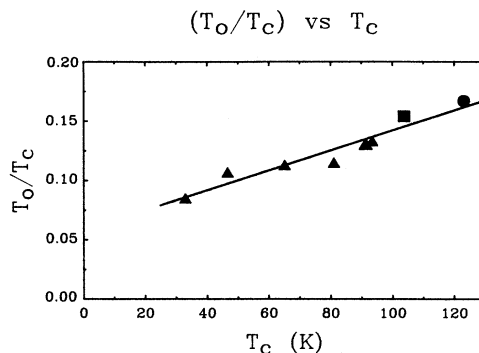


FIG. 11. From Fig. 10, the characteristic temperatures T_0 describing the temperature dependence of J_c . The ratio of T_0 to transition temperature T_c is shown vs T_c for Tl-2:2:2:3 (●) and Tl-2:1:2:2 (■) as well as a series of Fe-substituted $\text{YBa}_2(\text{Cu}_{1-x}\text{Fe}_x)_3\text{O}_z$ materials (▲).

materials, it is useful to examine what trends, if any, are evident in the characteristic temperature T_0 . This is presented in Fig. 11 as a plot of the ratio of (T_0/T_c) versus transition temperature T_c for Tl-based compounds as well as a series of Fe-substituted $\text{YBa}_2(\text{Cu}_{1-x}\text{Fe}_x)_3\text{O}_z$ compounds.¹⁷ The figure shows that the characteristic temperature T_0 increases proportionately faster than T_c , suggesting that the higher- T_c materials can be potentially usable at higher reduced temperatures $t = (T/T_c)$; this assumes that the calculated intragranular J_c values establish an upper bound on the realizable transport currents. Our results suggest, however, that application of large magnetic fields leads to a more rapid decrease of the intragranular J_c in these Tl-based materials than for Y-1:2:3. In light of this work, it is not presently possible to establish firm limits on the attainable current carrying properties of the Tl-based family of high- T_c compounds.

ACKNOWLEDGMENTS

Research sponsored by the Department of Materials Sciences, U. S. Department of Energy under Contract No. DE-AC05-84OR21400 with Martin Marietta Energy Systems, Inc.

¹Z. Z. Sheng and A. M. Hermann, *Nature* (London) **332**, 55 (1988); **332**, 138 (1988).

²C. C. Torardi, M. A. Subramanian, J. C. Calabrese, J. Gopalakrishnan, K. J. Morrissey, T. R. Askew, R. B. Flippen, U. Chowdhry, and A. W. Sleight, *Science* **240**, 631 (1988).

³M. A. Subramanian, J. C. Calabrese, C. C. Torardi, J. Gopalakrishnan, T. R. Askew, R. B. Flippen, K. J. Morrissey, U. Chowdhry, and A. W. Sleight, *Nature* (London) **332**, 420 (1988).

⁴R. M. Hazen, L. W. Finger, R. J. Angel, C. I. Prewitt, N. L. Ross, C. G. Hadidiacos, P. H. Heaney, D. R. Veblen, Z. Z. Sheng, and A. M. Hermann, *Phys. Rev. Lett.* **60**, 1657 (1988).

⁵C. C. Torardi, M. A. Subramanian, J. C. Calabrese, J.

Gopalakrishnan, E. M. McCarron, K. J. Morrissey, J. R. Askew, R. B. Flippen, U. Chowdhry, and A. W. Sleight, *Phys. Rev. B* **38**, 225 (1988).

⁶A. W. Hewat, E. A. Hewat, J. Brynestad, H. A. Mook, and E. D. Specht, *Physica A* **152**, 438 (1988).

⁷J. R. Clem and V. G. Kogan, *Jpn. J. Appl. Phys.* **26**, Suppl. 26-3, 1161 (1987).

⁸J. R. Thompson, S. T. Sekula, B. C. Sales, Y. C. Kim, D. K. Christen, J. Brynestad, and L. A. Boatner, in *Extended Abstracts: High Temperature Superconductors II*, edited by D. W. Capone II, W. H. Butler, B. Batlogg, and C. W. Chu (Materials Research Society, Pittsburgh, 1988), Vol. EA-14, p. 225.

⁹D. K. Christen, Y. C. Kim, S. T. Sekula, J. R. Thompson, B. C.

- Sales, L. A. Boatner, and J. D. Budai, IEEE Trans. Magn. (to be published).
- ¹⁰J. R. Clem, Physica C **153-155**, 50 (1988).
- ¹¹R. L. Peterson and J. W. Ekin, Phys. Rev. B **37**, 9848 (1988).
- ¹²R. B. Stephens, Cryogenics (to be published).
- ¹³H. Dersch and G. Blatter, Phys. Rev. B **38**, 11391 (1988).
- ¹⁴W. A. Fietz and W. W. Webb, Phys. Rev. **178**, 657 (1969).
- ¹⁵S. T. Sekula, D. K. Christen, H. R. Kerchner, J. R. Thompson, L. A. Boatner, and B. C. Sales, Jpn. J. Appl. Phys. **26**, Suppl. 26-3 1185 (1987).
- ¹⁶Y. Yeshurun and A. P. Malozemoff, Phys. Rev. Lett. **60**, 2202 (1988).
- ¹⁷S. T. Sekula, J. Brynstad, D. K. Christen, J. R. Thompson, and Y. C. Kim, IEEE Trans. Magn. (to be published).
- ¹⁸D. C. Larbalestier, S. E. Babcock, X. Cai, M. Daeumling, D. P. Hampshire, T. F. Kelly, L. A. Lavanier, P. J. Lee, and J. Seuntjens, Physica C **153-155**, 1580 (1988).
- ¹⁹D. K. Finnemore, J. E. Ostenson, L. Ji, R. W. McCallum, and J. R. Clem, in *Advances in Cryogenic Engineering*, edited by A. F. Clark and R. P. Reed (Plenum, New York, 1988), Vol. 34, p. 613.
- ²⁰S. Senoussi, M. Oussena, G. Collin, and I. A. Campbell, Phys. Rev. B **37**, 9792 (1988).
- ²¹H. K pfer, S. M. Green, C. Jiang, Yu Mei, H. L. Luo, R. Meier-Hirmer, and C. Politis, Z. Phys. B **71**, 63 (1988).
- ²²J. F. Kwak, E. L. Venturini, R. J. Baughman, B. Morosin, and D. S. Ginley, Physica C **156**, 103 (1988).